Available online at www.sciencedirect.com
SCIENCE DIRECT
Acta Materialia 53 (2005) 5439–5447
Acta MATERIALIA
www.actamat-journals.com

Thermal stability of retained austenite in TRIP steels studied by synchrotron X-ray diffraction during cooling

N.H. van Dijk [a,*], A.M. Butt [a,b], L. Zhao [b,c], J. Sietsma [b], S.E. Offerman [b], J.P. Wright [d], S. van der Zwaag [e]

[a] Fundamental Aspects of Materials and Energy, Faculty of Applied Sciences, Delft University of Technology, Mekelweg 15, 2629 JB Delft, The Netherlands
[b] Department of Materials Science and Engineering, Delft University of Technology, Rotterdamseweg 137, 2628 AL Delft, The Netherlands
[c] Netherlands Institute for Metals Research, Rotterdamseweg 137, 2628 AL Delft, The Netherlands
[d] European Synchrotron Radiation Facility, 6 Rue Jules Horowitz, BP 220, 38043 Grenoble Cedex, France
[e] Department of Aerospace Engineering, Delft University of Technology, Kluijverweg 1, 2629 HS Delft, The Netherlands

Received 30 May 2005; accepted 11 August 2005
Available online 30 September 2005

Abstract

We have performed in situ X-ray diffraction measurements at a synchrotron source in order to study the thermal stability of the retained austenite phase in transformation induced plasticity steels during cooling from room temperature to 100 K. A powder analysis of the diffraction data reveals a martensitic transformation of part of the retained austenite during cooling. The fraction of austenite that transforms during cooling is found to depend strongly on the bainitic holding time and the composition of the steel. It is shown that that austenite grains with a lower average carbon concentration have a lower stability during cooling.
© 2005 Acta Materialia Inc. Published by Elsevier Ltd. All rights reserved.

Keywords: TRIP steel; Synchrotron radiation; Martensitic phase transformation; Metastable phases

1. Introduction

Recently, low-alloyed transformation induced plasticity (TRIP) steels have attracted growing interest because of their high strength and good formability [1–3]. TRIP steels possess a multiphase microstructure containing ferrite (α-Fe), bainite, and (metastable) austenite (γ-Fe). The so-called TRIP effect in these steels arises from a martensitic transformation of the metastable retained austenite phase induced by external stress. It was found experimentally [4] and theoretically [5] that the austenite volume fraction, the carbon concentration in the austenite grains, and the grain size of the retained austenite play a crucial role in the TRIP properties as they significantly affect the mechanical stability of the retained austenite. Despite recent efforts, the understanding of the physical mechanism that controls the stability of the retained austenite in TRIP steels is still limited.

In previous experiments we have studied the volume fraction of retained austenite as a function of the chemical composition and the bainitic holding time by dilatometry [6], X-ray diffraction [7], and SQUID magnetisation [8]. The average austenite grain size was characterised by neutron depolarisation measurements [9]. By in situ X-ray diffraction measurements at a synchrotron source [10] we characterised the phase stability of the retained austenite under applied stress. These measurements allowed us to correlate the stability of the austenite grain to the relative orientation with respect to the applied stress.

An alternative way to study the phase stability of the retained austenite in TRIP steels with higher accuracy is to cool the material to low temperatures, and thereby increase the temperature-dependent chemical driving force for the martensitic transformation of the metastable retained austenite. In previous magnetisation measurements [11,12], we

* Corresponding author. Tel.: +31 15 27 86775; fax: +31 15 27 88303.
E-mail address: n.h.vandijk@tnw.tudelft.nl (N.H. van Dijk).

1359-6454/$30.00 © 2005 Acta Materialia Inc. Published by Elsevier Ltd. All rights reserved.
doi:10.1016/j.actamat.2005.08.017

have demonstrated that part of the retained austenite in TRIP steels can indeed become unstable during cooling. The grains with the lowest carbon concentration have the highest martensite start temperature (M_s) and are therefore expected to be relatively unstable during cooling [13]. The difference in thermal expansion of the ferrite matrix [14] and the austenite grains [15] can induce weak strains in the material during cooling, which may assist the martensitic transformation of the retained austenite.

In the current study, we performed in situ X-ray diffraction measurements at a synchrotron source to monitor the stability of retained austenite in TRIP steels during cooling. Part of the retained austenite phase is unstable when the material is cooled from room temperature to 100 K and transforms into martensite. In these measurements the austenite fraction and the average interstitial carbon concentration was monitored as a function of temperature for TRIP steels with different compositions and bainitic holding times. The analysis of the thermal stability of individual austenite grains will be the subject of a future paper.

2. Experimental

Three TRIP steels with different Al and P concentrations were studied. The chemical compositions of the $Al_{0.4}$, $Al_{0.4}P_{0.1}$, and $Al_{1.8}$ steels are listed in Table 1. Samples from the hot-rolled sheet material were machined into cylinders with a diameter of 0.50 mm and a length of 2.0 mm. The cylindrical axis of the sample was chosen along the rolling direction of the sheet material. The samples were heated in a salt bath to the intercritical holding temperature T_i listed in Table 2, to form a two-phase material containing austenite and ferrite. The intercritical holding temperature was selected to obtain a maximum fraction of retained austenite in the final material. The holding time at the intercritical annealing temperature was 30 min for all samples. After the intercritical annealing the samples were transferred to a second salt bath, held at the bainitic holding temperature T_{bh} indicated in Table 2. After bainitic holding times of 20, 60, 240, and 1000 s the samples were quenched in water. In Table 2, the transition temperatures and the equilibrium ferrite phase fraction at the intercritical annealing temperature, calculated with the thermodynamic database MTDATA, are also presented.

Table 1
Chemical composition of the studied steels (in wt.%) with balance Fe

Material	C	Mn	Si	Al	P
$Al_{0.4}$	0.188	1.502	0.254	0.443	0.015
$Al_{0.4}P_{0.1}$	0.175	1.493	0.255	0.439	0.102
$Al_{1.8}$	0.218	1.539	0.267	1.750	0.018

Table 2
The applied intercritical holding temperature T_i and the bainitic holding temperature T_{bh}

Material	T_i (K)	T_{bh} (K)	A_1^- (K)	A_1^+ (K)	A_3 (K)	f_γ^i (%)
$Al_{0.4}$	1073	673	967	983	1127	37
$Al_{0.4}P_{0.1}$	1028	673	969	984	1147	63
$Al_{1.8}$	1173	673	1016	1035	–	52

In addition, the thermodynamic transformation temperatures A_1^-, A_1^+, and A_3 together with the austenite fraction at the intercritical holding temperature f_γ^i calculated from the thermodynamic database MTData are listed. $Al_{1.8}$ steel in the pure austenite phase cannot be made.

X-ray diffraction measurements were performed using the three-dimensional X-ray diffraction microscope (3DXRD) at the beam line ID11 of the European Synchrotron Radiation Facility in transmission geometry. A monochromatic X-ray beam with an energy of 80 keV (wavelength of 0.155 Å) and a beam size of 39×39 μm^2 illuminated the 0.50 mm diameter of the cylindrical sample. The scattered intensity from both the retained austenite and the ferrite phase was recorded on a 2D detector placed behind the sample. During a 2 s exposure the sample was continuously rotated around the sample axis over an angle of 0.5°. By taking subsequent exposures an angular rotation range from +30° to −30° was covered. Due to the relatively small beam size and the limited angular rotation for each exposure the 2D diffraction patterns show separate reflections originating from individual austenite and ferrite grains.

The sample was glued on an invar rod to reduce movement due to temperature variations and cooled by a nitrogen gas cryostream cooler (Oxford Cryosystems) from 300 down to 100 K in steps of 20 K. After each temperature step the displacement of the sample with respect to the beam caused by the thermal contraction of the sample, the glue, and the invar rod was monitored by scans in the horizontal sample position, the vertical sample position, and the sample rotation angle. The intensity of a selected reflection from a characteristic individual ferrite grain in these scans was used to retrace exactly the same illuminated sample volume during the entire experiment.

3. Results

3.1. Diffracted intensity

In Fig. 1, the scattered intensity of the γ-{200}, γ-{220}, and γ-{311} austenite powder reflections is shown as a function of the scattering angle 2θ for the $Al_{0.4}$ steel with a bainitic holding time of $t_{bh} = 60$ s. The scattered intensity was obtained by adding all diffraction patterns for sample rotations in the angular range from −30° up to 30°. A radial average over constant scattering angles was performed to obtain 1D powder data from the individual reflections on the 2D diffraction patterns using the FIT2D software package [16]. In Fig. 1, the scattered intensity at room temperature is compared before and after cooling the sample to $T = 100$ K. A clear reduction in intensity is observed for all three austenite reflections, indicating that part of the retained austenite has indeed transformed during cooling. Since the relative change in intensity is approximately the same for all reflections we can conclude that the temperature-induced martensitic transformation of the retained

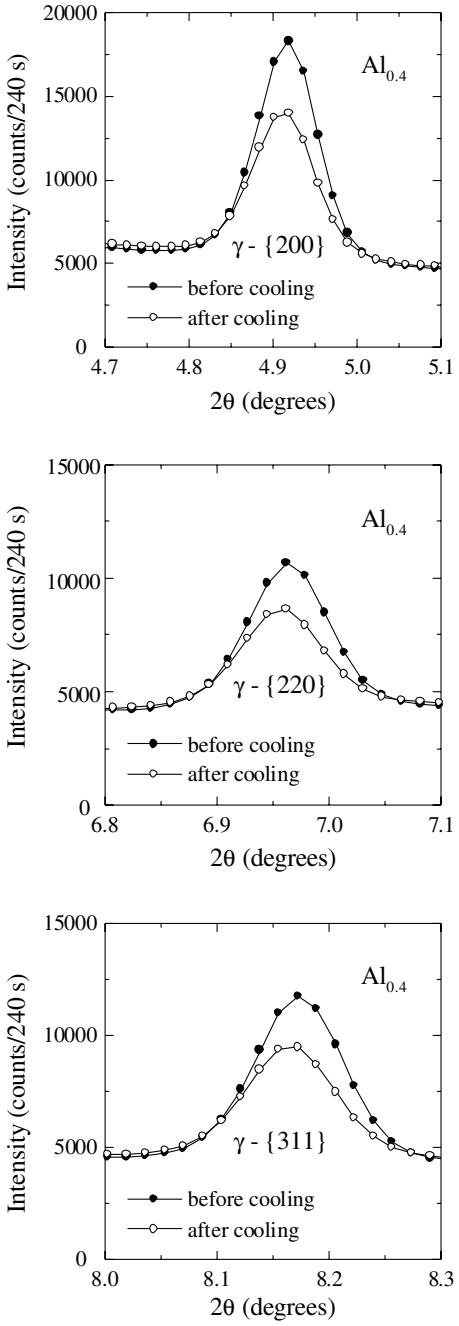

Fig. 1. Room temperature Bragg peak intensity of the γ-{200}, γ-{220}, and γ-{311} austenite powder peaks for the $Al_{0.4}$ steel with a bainitic holding time of $t_{bh} = 60$ s before (filled circles) and after (empty circles) cooling to 100 K. The cooling causes a martensitic transformation in part of the retained austenite and a change in the peak position.

austenite does not significantly influence the texture of the material. The reduction in scattered intensity of the austenite reflections is accompanied by an increase in the scattered intensity of the ferrite reflections (the small tetragonal distortion of martensite was indistinguishable from the body-centred cubic structure of ferrite). Furthermore, it is interesting to note that the position of the austenite peaks is shifted to lower scattering angles after cooling to 100 K, and subsequent reheating to room temperature. This indicates that the average austenite lattice parameter has increased due to a martensitic transformation of the retained austenite grains with the lowest interstitial carbon concentration. In order to monitor the stability of the retained austenite during cooling we analysed the scattered intensity for the face-centred cubic $\{200\}_\gamma$, $\{220\}_\gamma$, and $\{311\}_\gamma$ austenite (γ) reflections and the body-centred cubic $\{200\}_\alpha$, $\{211\}_\alpha$, and $\{220\}_\alpha$ ferrite (α) reflections. From the scattered intensity as a function of the scattering angle for each reflection, the integrated intensity and the mean scattering angle were obtained.

3.2. Volume fraction of retained austenite

The volume fraction of retained austenite f_γ was calculated from the integrated intensity of the austenite ($I_{\gamma,i}$) and ferrite ($I_{\alpha,i}$) peaks in the manner explained in Appendix A. The derived volume fraction of retained austenite at room temperature is shown in Table 3 before and after cooling to $T = 100$ K. The results for the $Al_{0.4}$ steel show that before cooling the highest fraction of retained austenite is obtained for a bainitic holding time of $t_{bh} = 60$ s. For this material the retained austenite is found to be the least stable during cooling as about a third of the original retained austenite is transformed into martensite during cooling to $T = 100$ K. For the longest bainitic holding time of $t_{bh} = 1000$ s virtually none of the original retained austenite transforms during cooling. The observed behaviour illustrates that during the bainitic holding the original austenite, formed during the intercritical annealing, continues to transform into bainite until only the most stable austenite remains. During the subsequent quench to room temperature the austenite is stabalised only for the longer bainitic holding times ($t_{bh} = 60$, 240, and 1000 s), while for the shortest bainitic holding time ($t_{bh} = 20$ s) the austenite is insufficiently enriched in carbon to be stabilised and part of the austenite is already transformed into martensite by the quench to room temperature. This leads to the observed maximum in the fraction retained austenite as a function of bainitic holding time. Consistent with the behaviour observed for the $Al_{0.4}$ steel with $t_{bh} = 60$ s, the $Al_{0.4}P_{0.1}$ and $Al_{1.8}$ steels with $t_{bh} = 60$ s, also show that about a third of the original retained austenite transforms into martensite during cooling. This suggests that the relative stability of the retained austenite during cooling is predominantly controlled by the kinetics of the bainite

Table 3
Volume fraction of retained austenite at room temperature before (f_γ^b) and after (f_γ^a) cooling to 100 K for different materials and bainitic holding times (t_{bh})

Material	t_{bh} (s)	f_γ^b (%)	f_γ^a (%)	f_γ^a/f_γ^b (%)
$Al_{0.4}$	20	6.32(7)	4.95(5)	78(1)
	60	7.49(5)	4.97(4)	66(1)
	240	6.01(5)	4.73(4)	79(1)
	1000	4.12(5)	3.98(3)	97(1)
$Al_{0.4}P_{0.1}$	60	5.83(5)	3.63(4)	62(1)
$Al_{1.8}$	60	7.71(6)	5.03(5)	65(1)

formation and the accompanying carbon enrichment of the austenite, which are similar in these materials.

In Fig. 2, the volume fraction of retained austenite is shown as a function of temperature for the $Al_{0.4}$ steel for different bainitic holding times. For all samples the steepest reduction in the volume fraction of retained austenite during cooling is observed for temperatures around 200 K. In Fig. 3, the volume fraction of retained austenite in the $Al_{0.4}$, $Al_{0.4}P_{0.1}$, and $Al_{1.8}$ steels with a bainitic holding time of $t_{bh} = 60$ s is shown as a function of temperature. The observed temperature dependence shows a close similarity for all three steels. The difference in composition seems to cause a shift in the original volume fraction of retained austenite. The original volume fraction of retained austenite is observed to decrease with additional phosphorus and to be relatively insensitive to the addition of aluminium.

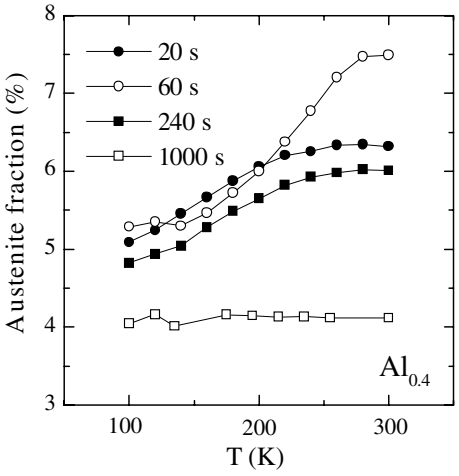

Fig. 2. Fraction retained austenite f_γ as a function of temperature T for $Al_{0.4}$ steels with bainitic holding times of $t_{bh} = 20$, 60, 240, and 1000 s during cooling from room temperature to 100 K.

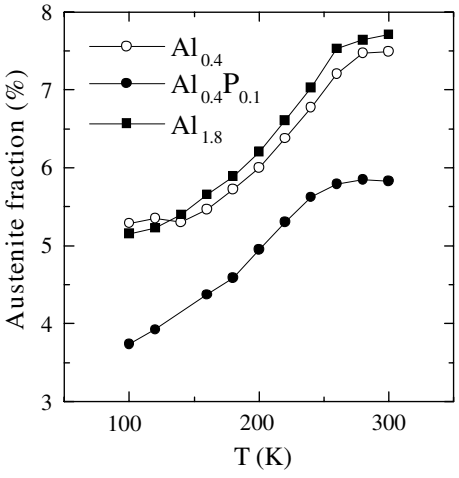

Fig. 3. Fraction retained austenite f_γ as a function of temperature T for $Al_{0.4}$, $Al_{0.4}P_{0.1}$, and $Al_{0.4}$ steels with a bainitic holding time of $t_{bh} = 60$ s during cooling from room temperature to 100 K.

3.3. Carbon concentration in retained austenite

The lattice parameter of the austenite (a_γ) and the ferrite (a_α) phases was determined from a fit of the peak positions of the monitored powder reflections to Bragg's law, according to the procedure described in Appendix B. The room temperature lattice parameters before and after cooling to 100 K are listed in Table 4. The changes in lattice parameter of the austenite phase reflect the difference in the average interstitial carbon concentration before and after cooling. At room temperature the best estimate of the compositional dependence of the austenite lattice parameter a_γ is given by [17,18]:

$$a_\gamma = 3.556 + 0.0453x_C + 0.00095x_{Mn} + 0.0056x_{Al}, \quad (1)$$

where a_γ is in Å and x_C, x_{Mn}, and x_{Al} are in wt.%. The influence of Si on the lattice parameter of austenite was found to be negligible within the experimental accuracy [18]. The influence of P on the lattice parameter of austenite has not been studied in detail and is also assumed to negligible. The corresponding room temperature lattice parameter of ferrite a_α amounts to [19]

$$a_\alpha = 2.8664 + 0.00055x_{Mn}, \quad (2)$$

where a_α is in Å and x_C and x_{Mn} in wt.%. Within the present experiment the martensite, which is formed from the meta-stable austenite during cooling, cannot be distinguished from the original ferrite matrix. The dissolved carbon causes a small tertagonal distortion of the martensite phase α' with respect to the lattice structure of the ferrite phase α . The martensite lattice parameters $a_{\alpha'}$ and $c_{\alpha'}$ correspond to [17]:

$$\begin{aligned} a_{\alpha'} &= a_\alpha - 0.014x_C, \\ c_{\alpha'} &= a_\alpha + 0.115x_C, \end{aligned} \quad (3)$$

where a_α, $a_{\alpha'}$, and $c_{\alpha'}$ are in Å and x_C is in wt.%. For a typical carbon concentration of about 1 wt.% the average martensite lattice parameter $(a_{\alpha'}^2 c_{\alpha'})^{1/3}$ only differs about 0.3% from the ferrite lattice parameter a_α. As the amount of retained austenite that transforms into martensite during cooling is relatively small compared to the phase fraction of the original ferrite phase, no distinction between the ferrite and the martensite is made in the analysis of the average carbon concentration in the retained austenite.

In our analysis the lattice parameter of the austenite was monitored relative to that of the ferrite phase (a_γ/a_α) in

Table 4
Average lattice parameter of retained austenite a_γ and ferrite a_α at room temperature before (index b) and after (index a) cooling to 100 K for different materials and bainitic holding times (t_{bh})

Material	t_{bh} (s)	a_γ^b (Å)	a_γ^a (Å)	a_α^b (Å)	a_α^a (Å)
$Al_{0.4}$	20	3.6063(1)	3.6067(1)	2.8673(1)	2.8665(1)
	60	3.6097(1)	3.6130(1)	2.8684(1)	2.8693(1)
	240	3.6065(1)	3.6072(1)	2.8652(1)	2.8646(1)
	1000	3.6142(2)	3.6145(1)	2.8692(1)	2.8694(1)
$Al_{0.4}P_{0.1}$	60	3.6018(1)	3.6060(1)	2.8655(1)	2.8671(1)
$Al_{1.8}$	60	3.6168(1)	3.6244(1)	2.8704(1)	2.8717(1)

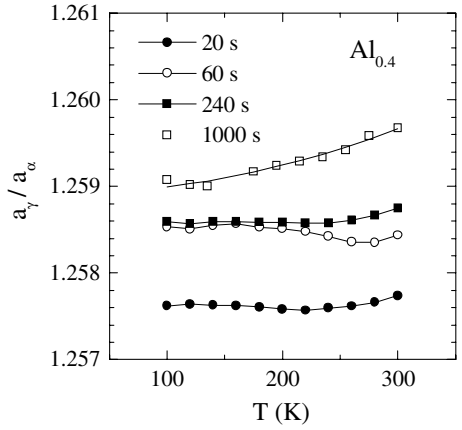

Fig. 4. Relative lattice parameter a_γ/a_α of the austenite phase (a_γ) divided by the ferrite phase (a_α) as a function of temperature T for the $Al_{0.4}$ steel with bainitic holding times of $t_{bh} = 20$, 60, 240, and 1000 s during cooling from room temperature to 100 K. The solid line for $t_{bh} = 1000$ s corresponds to a fit of the data that describes the difference in thermal contraction of the austenite and ferrite phase in the absence of a martensitic transformation (see text).

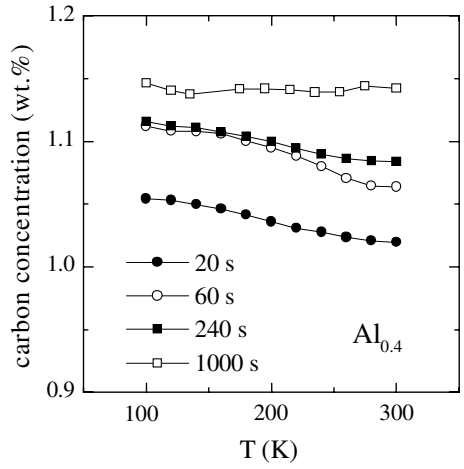

Fig. 5. Average carbon concentration in the austenite phase $\langle x_C \rangle$ as a function of temperature T for $Al_{0.4}$ steels with bainitic holding times of $t_{bh} = 20$, 60, 240, and 1000 s during cooling from room temperature to 100 K.

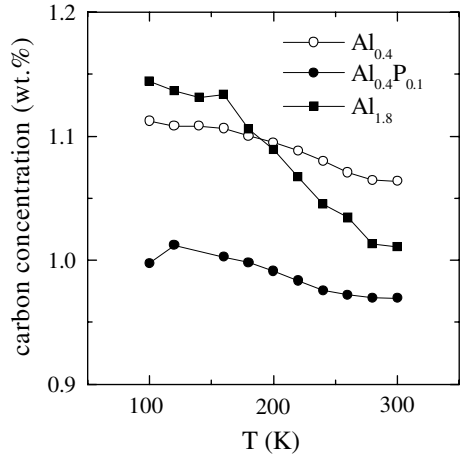

Fig. 6. Average carbon concentration in the austenite phase $\langle x_C \rangle$ as a function of temperature T for $Al_{0.4}$, $Al_{0.4}P_{0.1}$, and $Al_{0.4}$ steels with a bainitic holding time of $t_{bh} = 60$ s during cooling from room temperature to 100 K.

order to avoid an influence of small variations in the sample-detector distance, caused by sample displacements during cooling. In Fig. 4, the relative lattice parameter a_γ/a_α is shown as a function of temperature for the $Al_{0.4}$ steel with different bainitic holding times during cooling from room temperature to 100 K. The temperature dependence of a_γ/a_α is expected to depend on the average interstitial carbon concentration in the austenite phase and the difference in thermal expansion between the austenite and ferrite phase. As observed in Fig. 2 and Table 3, the $Al_{0.4}$ steel with the longest bainitic holding time ($t_{bh} = 1000$ s) shows virtually no martensitic transformation of the retained austenite during cooling. For this steel the observed temperature dependence of the relative lattice parameter a_γ/a_α is therefore caused entirely by the difference in thermal contraction of the austenite and ferrite phases. The behaviour observed for the $Al_{0.4}$ steel with $t_{bh} = 1000$ s can now be used for the other measurements to extract the change in lattice parameter caused by the enhanced average carbon contribution during cooling, as discussed in Appendix C.

In Fig. 5, the derived average carbon concentration in the retained austenite is shown as a function of temperature during cooling from room temperature to 100 K for the $Al_{0.4}$ steel with different bainitic holding times. It is remarkable that the sample with $t_{bh} = 20$ s shows the lowest carbon concentration, while the sample with $t_{bh} = 60$ s shows the largest increase in carbon concentration during cooling. The relatively large increase in carbon concentration observed for the sample with $t_{bh} = 60$ s coincides with the relatively large part of the initial volume fraction of retained austenite that is transformed into martensite during cooling.

In Fig. 6, the average carbon concentration in the austenite phase is shown as a function of temperature during cooling from room temperature to 100 K for the $Al_{0.4}$, $Al_{0.4}P_{0.1}$, and $Al_{1.8}$ steels with a bainitic holding time of $t_{bh} = 60$ s. The $Al_{1.8}$ steel shows the largest increase during cooling, while the relative increase is comparable for the $Al_{0.4}$ and $Al_{0.4}P_{0.1}$ steels. In Table 5, the average carbon concentration in the austenite phase, which has been derived from the room temperature lattice parameter before and after cooling to 100 K, is listed. The results are in good agreement with the temperature dependent results shown in Figs. 5 and 6. In Table 5, the amount of carbon present in the retained austenite $f_\gamma\langle x_C \rangle$ is listed relative to the nominal carbon concentration x_C^0 present in the steel. It is interesting to note that before cooling to 100 K large differences in the relative carbon content dissolved in the retained austenite $f_\gamma\langle x_C \rangle / x_C^0$ are observed, while after cooling for all steels about a quarter of the available carbon (x_C^0) remains present within the untransformed retained austenite ($f_\gamma\langle x_C \rangle$).

Table 5
Average carbon concentration $\langle x_C \rangle$ in retained austenite at room temperature before ($\langle x_C \rangle^b$) and after ($\langle x_C \rangle^a$) cooling to 100 K

Material	t_{bh} (s)	$\langle x_C \rangle^b$ (wt.%)	$\langle x_C \rangle^a$ (wt.%)	$f_\gamma^b \langle x_C \rangle^b / x_C^0$ (%)	$f_\gamma^a \langle x_C \rangle^a / x_C^0$ (%)
$Al_{0.4}$	20	1.020(3)	1.050(3)	34.3(4)	27.7(3)
	60	1.064(2)	1.111(3)	42.4(3)	29.4(2)
	240	1.084(3)	1.113(3)	34.6(3)	28.0(3)
	1000	1.142(5)	1.143(3)	25.0(3)	24.2(2)
$Al_{0.4}P_{0.1}$	60	0.969(3)	1.017(3)	32.3(3)	21.1(2)
$Al_{1.8}$	60	1.011(2)	1.147(3)	35.8(3)	26.5(2)

The value of $f_\gamma \langle x_C \rangle / x_C^0$ represents the fraction of the available carbon that is dissolved in the retained austenite before ($f_\gamma^b \langle x_C \rangle^b / x_C^0$) and after ($f_\gamma^a \langle x_C \rangle^a / x_C^0$) cooling to 100 K. In the presence of a compressive strain in the austenite phase of $\Delta\varepsilon_\gamma = 0.08\%$ for the $Al_{0.4}$ sample with $t_{bh} = 20$ s the effective carbon concentration is 0.06 wt.% higher than estimated directly from the austenite lattice parameter (see text).

4. Discussion

In Fig. 7, the average carbon concentration in the retained austenite phase $\langle x_C \rangle$ is plotted as a function of the volume fraction retained austenite f_γ for the $Al_{0.4}$ steel with different bainitic holding times during cooling. The results are consistent with our previous observations that the average carbon concentration within the austenite phase increases when the austenite fraction decreases. It is remarkable that the temperature dependent data for the samples with the longer bainitic holding times $t_{bh} = 60$, 240, and 1000 s can all be described by a single linear relation:

$$\langle x_C \rangle = C_0 - C_1 f_\gamma, \tag{4}$$

where $\langle x_C \rangle$ is in wt.%, f_γ is in volume %. The fit parameters C_0 and C_1 for the $Al_{0.4}$ steel with a bainitic holding time of $t_{bh} = 60$ s are listed in Table 6. As indicated by the dashed line in Fig. 7 the samples with a bainitic holding time of $t_{bh} = 240$ and 1000 s closely follow the same linear relation. However, the sample with the shortest bainitic holding time, $t_{bh} = 20$ s, shows a clear deviation from this common linear relation. Although the slope for the sample with $t_{bh} = 20$ s is the same as for the samples with a higher bainitic holding time, a clear offset of about 0.06 wt.% carbon is observed with respect to the linear relation indicated by the dashed line in Fig. 7. The most likely origin for this offset

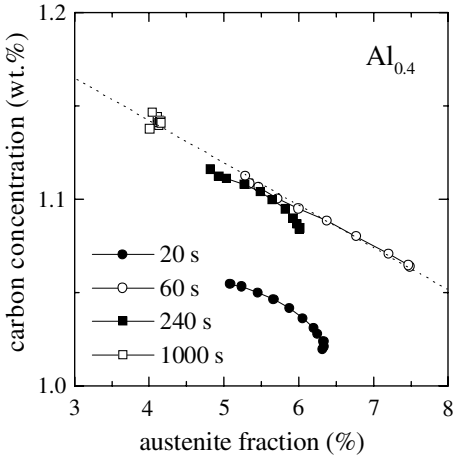

Fig. 7. Average carbon concentration of the austenite phase as a function of the fraction retained austenite f_γ for $Al_{0.4}$ steels with bainitic holding times of $t_{bh} = 20$, 60, 240, and 1000 s during cooling from room temperature to 100 K. The dashed line is a fit to the data (see text).

seems the formation of an isotropic compressive strain during the temperature quench from the bainitic holding temperature to room temperature. In this case the magnitude of the isotropic compressive strain within the austenite phase can be estimated with the help of Eq. (1) and amounts to $\Delta\varepsilon_\gamma = 0.08\%$. For the sample with the shortest bainitic holding time ($t_{bh} = 20$ s) a relatively small amount of bainite is formed and the enrichment in carbon of the austenite is relatively low during the bainitic holding. As a consequence, part of the original austenite grain already transforms into martensite during the quench to room temperature, causing a strain in the remaining part (or parts) of the austenite grain. For longer bainitic holding times ($t_{bh} = 60$, 240, and 1000 s) more bainite is formed, the remaining austenite is more enriched in carbon, and the austenite is stable in the quench to room temperature. During the temperature-induced martensitic transformation during cooling, complete grains of retained austenite are expected to transform. In this case the martensitic transformation of one austenite grain will not induce a significant strain in a neighboring austenite grain.

The temperature-dependent data of the $Al_{0.4}P_{0.1}$ and $Al_{1.8}$ steels with a bainitic holding time of $t_{bh} = 60$ s can also be described by a linear relation. The parameters obtained from a fit to Eq. (4) are listed in Table 6. About the same slope (C_1) is observed for the $Al_{0.4}P_{0.1}$ steel as for the $Al_{0.4}$ steel, while for the $Al_{1.8}$ steel a significantly higher value is obtained.

In Fig. 8, the main results of the effect of cooling on the $Al_{0.4}$ steel with different bainitic holding times are summarised. Before cooling a maximum in the volume fraction of retained austenite as a function of the bainitic holding time is observed. The highest volume fraction of retained austenite was found for a bainitic holding time of $t_{bh} = 60$ s. This sample with the highest initial volume fraction of

Table 6
Fit parameters C_0 and C_1 to the linear relation of Eq. (4) between the average carbon concentration in the austenite phase $\langle x_C \rangle$ and the austenite volume fraction f_γ for the steels with a bainitic holding time of $t_{bh} = 60$ s during cooling to $T = 100$ K

Material	t_{bh} (s)	C_0 (wt.%)	C_1 (wt.%/vol.%)
$Al_{0.4}$	60	1.219(2)	0.0207(4)
$Al_{0.4}P_{0.1}$	60	1.099(2)	0.0221(4)
$Al_{1.8}$	60	1.41(1)	0.051(2)

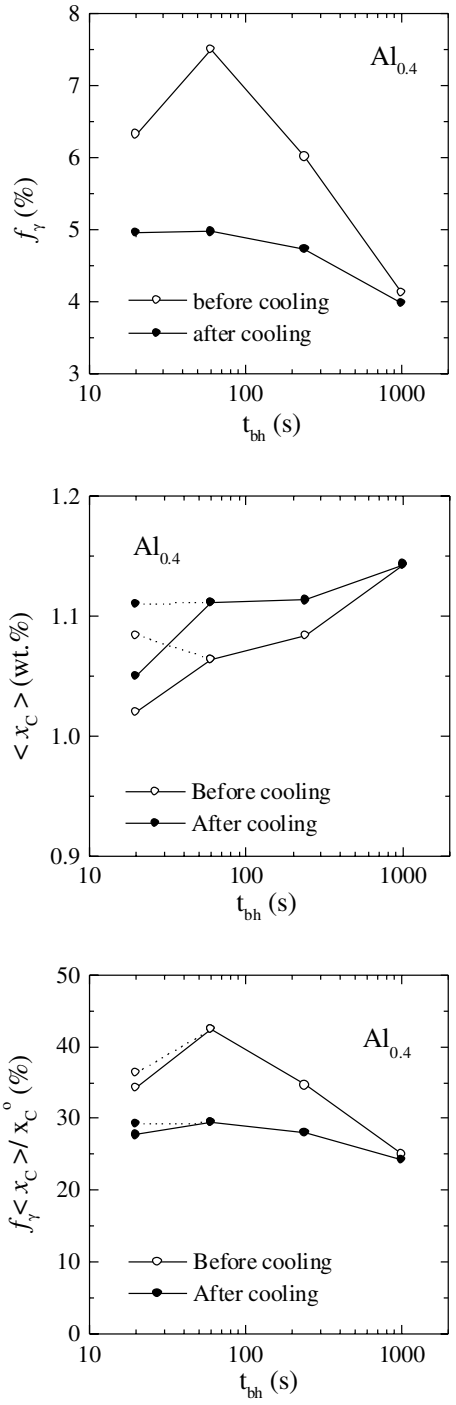

Fig. 8. Volume fraction f_γ (a), average carbon concentration $\langle x_C \rangle$ (b), and dissolved carbon fraction $f_\gamma \langle x_C \rangle / x_C^0$ (c) of the retained austenite phase as a function of the bainitic holding time t_{bh} for the $Al_{0.4}$ steel at room temperature before and after cooling to 100 K. The dashed lines indicate the results when a compressive strain of $\Delta\varepsilon_\gamma = 0.08\%$ is assumed for the austenite phase for the sample with $t_{bh} = 20$ s (see text).

retained austenite was also the most unstable during cooling (about a third of the initial retained austenite transformed). For the sample with the longest bainitic holding time, $t_{bh} = 1000$ s, virtually no austenite is transformed into martensite by cooling to 100 K. The average carbon concentration in the retained austenite further shows a non-monotonic dependence on the bainitic holding time. After cooling all samples show an increase in the average carbon concentration in the retained austenite. The largest increase in carbon concentration is observed for the most unstable sample with $t_{bh} = 60$ s. When a compressive strain of $\Delta\varepsilon_\gamma = 0.08\%$ in the austenite phase is assumed for the sample with $t_{bh} = 20$ s, the actual carbon concentration is 0.06 wt.% higher than estimated directly from the austenite lattice parameter. The influence of such a strain is indicated by the dashed lines in Fig. 8. In the absence of a compressive strain in the austenite for the sample with $t_{bh} = 20$ s the stability of the austenite cannot be directly related to the average carbon concentration in the retained austenite, indicating that the carbon concentration is possibly not the only significant parameter that controls the stability of the retained austenite. If a compressive strain is assumed for the sample with $t_{bh} = 20$ s, the sample with the lowest carbon concentration before cooling ($t_{bh} = 60$ s) is the least stable during cooling and the samples with the shorter bainitic holding times of $t_{bh} = 20$, 60, and 240 s, all show the same carbon concentration of $x_C \approx 1.11$ wt.% carbon after cooling.

According to Andrews' empirical relation between the composition and the onset of the martensitic transformation [13] the martensite start temperature M_s scales with the average carbon concentration in the retained austenite x_C:

$$M_s = M_{so} - Ax_C, \tag{5}$$

where M_s is in K, x_C is in wt.%, $A = 425$ K/wt.%, $M_{so} = 764$ K for the $Al_{0.4}$ and $Al_{0.4}P_{0.1}$ steels, and $M_{so} = 762$ K for the $Al_{1.8}$ steel [20]. This relation predicts that austenite grains with a carbon concentration of $x_C > 1.1$ wt.% are stable at $T = 300$ K. Upon cooling to $T = 100$ K the austenite grains with a carbon concentration of 1.1 wt.% $< x_C < 1.5$ wt.% are expected to transform into martensite. However, as shown in Tables 3 and 5, we find a stable volume fraction of retained austenite after cooling to 100 K with average carbon concentrations ranging from 1.05 up to 1.15 wt.%. This suggests that the empirical relation given in Eq. (1) has a limited validity for our TRIP steels (especially at low temperatures), and that parameters other than chemical composition also play a significant role in the stability of the austenite grains. To be fair, it should be noted that the Andrews' relation was derived for the transformation of fully austenitic starting materials and not for isolated austenitic islands in a non-austenitic matrix.

As shown in Fig. 8, the fraction of carbon stored in the retained austenite $f_\gamma \langle x_C \rangle / x_C^0$ before cooling shows a maximum for the sample with a bainitic holding time of $t_{bh} = 60$ s. After cooling to 100 K this maximum in $f_\gamma \langle x_C \rangle / x_C^0$ is however much less pronounced and a value of about a quarter is found for all bainitic holding times. It would be interesting to correlate the stability of the austenite grains also to the size of the austenite grains to see whether either small or large grains predominantly transform during cooling to 100 K. From our present powder

analysis, we cannot obtain information on the grain size, but a future study aimed at analysing individual reflections originating from single austenite grains, will make it possible to obtain the particle size distribution of the austenite grains as a function of temperature as well.

5. Conclusions

We have performed in situ X-ray diffraction measurements in order to study the thermal stability of the retained austenite phase in TRIP steels during cooling from room temperature to 100 K. A powder analysis of the data shows the general characteristics of the austenite to martensite transformation during cooling. The prime conclusions are:

1. Part of the initial retained austenite formed in the TRIP steels was found to transform into martensite during cooling, while another part remained stable down to the lowest temperature reached. The fraction of retained austenite that transforms during cooling strongly depends on the bainitic holding time and the composition. For the longest bainitic holding time virtually no retained austenite transformed during cooling. Apparently, only the most stable austenite grains remain after the long bainitic holding time of $t_{bh} = 1000$ s.
2. Austenite grains with a lower carbon concentration have a lower stability during cooling for all studied samples. The average carbon concentration in the untransformed retained austenite after cooling was higher than the average carbon concentration before cooling.
3. For the $Al_{0.4}$ steel with the longer bainitic holding times of $t_{bh} = 60$, 240, and 1000 s all data for the average carbon concentration in the retained austenite phase as a function of the austenite fraction fall on a single straight line.
4. For the $Al_{0.4}$ steel with the shortest bainitic holding time of $t_{bh} = 20$ s the temperature stability of the austenite phase can only be understood when a compressive strain of $\Delta\varepsilon_\gamma = 0.08\%$ in the austenite phase is assumed.

Acknowledgements

We acknowledge the European Synchrotron Radiation Facility for provision of synchrotron radiation facilities and we would like to thank L. Margulies for assistance in using beamline ID11. This work was financially supported in part by the Foundation for Fundamental Research on Matter (FOM) of the Netherlands Organisation for Scientific Research (NWO) and the Netherlands Institute for Metals Research (NIMR).

Appendix A. Volume fraction of retained austenite

The volume fraction of retained austenite f_γ was estimated from the integrated intensity of the monitored austenite ($I_{\gamma,i}$) and ferrite ($I_{\alpha,i}$) peaks:

$$f_\gamma = \frac{\frac{1}{N}\sum_{i=1}^{N}\left(\frac{I_{\gamma,i}}{R_{\gamma,i}}\right)}{\frac{1}{N}\sum_{i=1}^{N}\left(\frac{I_{\gamma,i}}{R_{\gamma,i}}\right) + \frac{1}{M}\sum_{i=1}^{M}\left(\frac{I_{\alpha,i}}{R_{\alpha,i}}\right)}, \tag{A1}$$

where N and M are the number of considered austenite and ferrite reflections, respectively. The index i refers to the $\{hkl\}$ reflection of interest. The normalisation factors for the austenite ($R_{\gamma,i}$) and ferrite ($R_{\alpha,i}$) peak intensities are obtained from the diffracted intensity from a powder without texture $I_{th,i}$:

$$R_i = \frac{I_{th,i}}{\Phi_0 V \mu}, \tag{A2}$$

where Φ_0 is the incident photon flux, V the illuminated sample volume, and μ the sample transmission ($\mu = 0.80$ for a sample thickness of 0.50 mm and an X-ray energy of 80 keV). The predicted diffracted intensity of a complete powder ring $I_{th,i}$ amounts to [21,22]:

$$I_{th,i} = \Phi_0 r_0^2 \frac{m_{hkl}\lambda^3 |F_{hkl}|^2 V}{v^2} \mu L_p P \exp(-2M), \tag{A3}$$

where $r_0 = 2.82 \times 10^{-15}$ m is the Thomson scattering length, m_{hkl} the multiplicity factor, $\lambda = 0.155$ Å the photon wavelength ($E = 80$ keV), F_{hkl} the structure factor, v the volume of the unit cell, $L_p = 1/4\sin(\theta)$ is the Lorentz factor for the complete powder ring, $P = [1 + \cos^2(2\theta)]/2$ the polarisation factor, and $\exp(-2M)$ is the Debye–Waller factor. At $T = 300$ K the normalisation factors are estimated at $R_{\gamma,\{200\}} = 2.067$ m^{-1}, $R_{\gamma,\{220\}} = 1.796$ m^{-1}, $R_{\gamma,\{311\}} = 2.282$ m^{-1}, $R_{\alpha,\{200\}} = 1.269$ m^{-1}, $R_{\alpha,\{211\}} = 2.932$ m^{-1}, and $R_{\alpha,\{220\}} = 0.951$ m^{-1}. At lower temperatures the normalisation factors show a slight increase until about 5% higher values are reached at $T = 100$ K.

Appendix B. Lattice parameters of austenite and ferrite

The mean lattice parameter a for the austenite and ferrite phases can be determined from the experimental mean scattering angle $2\theta_i$ of the considered $\{hkl\}$ reflections using the following relation:

$$a = \frac{1}{N}\sum_{i=1}^{N}\left(\frac{\lambda}{2}\right)\frac{\sqrt{h^2+k^2+l^2}}{\sin(\theta_i)}, \tag{B1}$$

where N is the number of considered reflections for the austenite or ferrite phase. The scattering angles were calibrated by the powder pattern of LaB_6.

Appendix C. Average carbon concentration in retained austenite

In the absence of a martensitic transformation of the retained austenite the temperature dependence of the austenite lattice parameter a_γ and the ferrite lattice parameter a_α are governed by their coefficient of the linear thermal expansion $\alpha = (1/a)(da/dT)$. The room temperature literature values of $\alpha_\alpha = 11.7 \times 10^{-6}$ K^{-1} [14] for ferrite and $\alpha_\gamma = 24.1 \times 10^{-6}$ K^{-1} [15] for austenite reflect the difference

in phonon spectrum of the ferrite and austenite phases characterised a Debye temperature of $\theta_D = 430$ K for ferrite [23] and $\theta_D = 335$ K for austenite [24]. Lu and coworkers [25] have evaluated the thermal expansion of a large number of cubic metals as a function of temperature and analysed them in terms of the Debye–Grüneisen model. In the temperature range of interest for our experiments the thermal expansion of the austenite and ferrite phases is expected to behave roughly linear with temperature:

$$\alpha(T) \approx \alpha(300)\left(\frac{T}{300}\right), \tag{C1}$$

where the temperature T in K and α (300) is the thermal expansion at $T = 300$ K. As a result the temperature dependence of the lattice parameter is given by:

$$a(T) \approx a(0)\left(1 + \frac{1}{2}\alpha(300)\left(\frac{T^2}{300}\right)\right). \tag{C2}$$

The corresponding temperature dependence of the relative lattice parameter a_γ/a_α is then given by:

$$\left(\frac{a_\gamma}{a_\alpha}\right)(T) \approx \left(\frac{a_\gamma}{a_\alpha}\right)(0)\left(1 + \frac{1}{2}(\alpha_\gamma(300) - \alpha_\alpha(300))\left(\frac{T^2}{300}\right)\right). \tag{C3}$$

In our experiment we have used the experimental data of a_γ/a_α as a function of temperature for the $Al_{0.4}$ steel with a bainitic holding time of $t_{bh} = 1000$ s (Fig. 4) to estimate the difference in thermal expansion between the austenite and ferrite phase because this sample shows virtually no martensitic transformation of the retained austenite during cooling. Based on Eq. (C3) the experimental data in Fig. 4 for a_γ/a_α are fitted by:

$$\left(\frac{a_\gamma}{a_\alpha}\right)_{\text{fit}}(T) = A + BT^2, \tag{C4}$$

with $A = 1.25891(3)$ and $B = 8.36(53) \times 10^{-9}\ \text{K}^{-2}$. The resulting estimate for the difference in thermal expansion between the austenite and ferrite phase amounts to $\alpha_\gamma(300) - \alpha_\alpha(300) = 4.0 \times 10^{-6}\ \text{K}^{-1}$, which is somewhat smaller than expected from the reported literature values. This is probably caused by the fact that the reported coefficient of the linear thermal expansion for austenite $\alpha_\gamma = 24.1 \times 10^{-6}\ \text{K}^{-1}$ [15] corresponds to an average value in the temperature range from 298 to 603 K, and is therefore representative for an average temperature of 450 K. Assuming a linear temperature dependence for the thermal expansion of austenite, an estimated value of $\alpha_\gamma(300) = (300/450) \times \alpha_\gamma(450) = 16.0 \times 10^{-6}\ \text{K}^{-1}$ is obtained at $T = 300$ K. The corresponding difference in thermal expansion between the austenite and the ferrite phase at room temperature α_γ (300) $- \alpha_\alpha(300) = 4.3 \times 10^{-6}\ \text{K}^{-1}$ is in good agreement with our present experimental result. The difference in the relative thermal contraction between austenite and ferrite accumulates to $\Delta\varepsilon(T) = (300/2)[\alpha_\gamma(300) - \alpha_\alpha(300)][1 - (T/300)^2] = 0.053\%$ at 100 K. The effective strain within the austenite grains caused by the difference in thermal contraction is expected to be significantly smaller since a significant part is accommodated by the matrix composed of ferrite and bainite.

We have multiplied all experimental curves of a_γ/a_α versus temperature by $(a_\gamma/a_\alpha)_{\text{fit}}(300)/(a_\gamma/a_\alpha)_{\text{fit}}(T)$ to obtain a relative lattice parameter that can be compared directly to $(a_\gamma/a_\alpha)(300)$ from the literature data the room temperature lattice parameters of ferrite a_α Eq. (2) and of austenite a_γ Eq. (1). From this comparison the interstitial carbon concentration in the austenite phase is obtained.

References

[1] Wang X, Wang S, Hua L. J Mater Sci Technol 1995;11:440.
[2] Sugimoto K, Kobayashi M, Yasuki S. Metall Mater Trans A 1997;28A:2637.
[3] De Cooman BC. Curr Opin Solid State Mater Sci 2004;8:285.
[4] Bleck W, Hulka K, Papamentellos K. Mater Sci Forum 1998;284–286:327.
[5] Haidemenopoulos GN, Vasilakos AN. Steel Res 1996;67:513.
[6] Zhao L, Kop TA, Rolin V, Sietsma J, Mertens A, Jacques PJ, et al. J Mater Sci 2002;37:1585.
[7] Zhao L, Sietsma J, van der Zwaag S. Proc Euro Conf Mater Sci. Weinheim: Wiley–VCH; 2000. p. 77.
[8] Zhao L, van Dijk NH, Brück E, Sietsma J, van der Zwaag S. Mater Sci Eng A 2001;A313:145.
[9] van Dijk NH, Zhao L, Rekveldt MTh, Fredrikze H, Tegus O, Brück E, et al. Phys B 2004;350:e463.
[10] Kruijver SO, Zhao L, Sietsma J, Offerman SE, van Dijk NH, Margulies L, et al. Steel Res 2002;73:236.
[11] Zhao L, Tegus O, Brück E, van Dijk NH, Kruijver S, Sietsma J, et al. In: De Cooman DC, editor. Proceedings international conference on TRIP-aided high strength ferrous alloys, Gent, Belgium, 19–21 June 2002, Aachen: Wissenschaftsverlag Mainz; 2002. p. 71.
[12] Ref. [11] reports that all of the retained austenite transforms during cooling from 300 to 5 K. This statement was based on X-ray diffraction measurements, which did not show retained austenite after cooling. A later comparison of the saturation magnetisation of the TRIP steel to the value of the as-received material (based on the method described in [8]), however indicates that the original volume fraction of retained austenite amounted to $f_\gamma = 10.2\%$ (in agreement with the X-ray data before cooling). From this initial austenite fraction only 2.3% transformed into martensite during cooling to 5 K according to the magnetisation measurements.
[13] Andrews KW. J Iron Steel Inst Jpn 1965;7:721.
[14] Ashcroft NW, Mermin ND. Solid state physics. Philadelphia (PA): Saunders College; 1976.
[15] Choi SD, Kim HS, Je JH, Park SH. J Mater Sci Lett 2002;21:353.
[16] Hammersley AP, Svensson SO, Hanfland M, Fitch AN, Häusermann D. High Pressure Res 1996;14:235.
[17] Cheng L, Böttger A, de Keijser ThH, Mittemeijer EJ. Scripta Mater 1990;24:509.
[18] Dyson DJ, Holmes B. J Iron Steel Inst 1970;208:469.
[19] Li C-M, Sommer F, Mittemeijer EJ. Mater Sci Eng A 2002;A325:307.
[20] Zhao L, Moreno J, Kruijver S, Sietsma J, van der Zwaag S. In: De Cooman DC, editor. Proceedings international conference on TRIP-aided high strength ferrous alloys, Gent, Belgium, 19–21 June 2002, Aachen: Wissenschaftsverlag Mainz; 2002. p. 141.
[21] Als-Nielsen J, McMorrow D. Elements of modern X-ray physics. Chichester: Wiley; 2001.
[22] Warren BE. X-ray diffraction. New York (NY): Dover Publications; 1990.
[23] Jarestky J, Stassis C. Phys Rev B 1987;35:4500.
[24] Matsumura O, Sakuma Y, Takechi Y. Scripta Metall 1987;21:1301.
[25] Lu X-G, Selleby M, Sundman B. Acta Mater 2005;53:2259.